



Cite this: DOI: 10.1039/d6py00397d

Ring-opening copolymerization of (dihydro) levoglucosenone-derived spiro-epoxides and cyclic anhydrides

Tianle Gao,^{†a} Hiroto Ayakawa,^{†b} Tatsuya Nishimura,^{id c} Ayano Yoshida,^b Moeno Sugiyama,^b Takuya Yamamoto,^{id a} Kenji Tajima,^{id a} Kenji Takahashi,^{id d} Feng Li,^{id *a} Takuya Isono,^{id a} Katsuhiko Maeda^{id e} and Toshifumi Satoh^{id *a,f,g}

Ring-opening copolymerization (ROCOP) of epoxides with cyclic anhydrides is a powerful strategy for synthesis of structure-controlled polyesters with tunable properties. Although considerable efforts have been devoted to expanding the monomer scope by introducing specific side groups or utilizing new biomass-derived feedstocks, the influence of monomer substitution patterns has received far less attention. In particular, in contrast to the well-studied mono- and 1,2-disubstituted epoxides, 1,1-disubstituted epoxides have been much less explored. Herein, we report cellulose-derived spiro-epoxides DBOO and DBOOPh as a new class of 1,1-disubstituted epoxide monomers for ROCOP with cyclic anhydrides. ROCOP of DBOO with phthalic anhydride proceeds in a living/controlled manner, affording polyesters with predominantly alternating structures, as confirmed by NMR and MALDI-TOF MS analyses. By varying the monomer combinations, a series of polyesters bearing spirocyclic backbones were synthesized. Thermal analyses revealed sufficient thermal stability and widely tunable glass-transition temperatures ranging from 29 to 130 °C. Moreover, the chirality of DBOO and DBOOPh induced chiral environments along the polymer chain, as evidenced by the circular dichroism spectra of the resulting polyesters. It may further induce the polymer chains to adopt a biased one-handed helical conformation. This work not only expands the monomer scope of ROCOP to biomass-derived spiro-epoxides, thus providing access to polyesters with unique rigid spirocyclic backbones, but also demonstrates the potential of polyesters synthesized *via* ROCOP as new chiral materials.

Received 24th April 2026,
Accepted 2nd June 2026

DOI: 10.1039/d6py00397d

rsc.li/polymers

1. Introduction

Polyesters constitute one of the most important classes of polymeric materials owing to their structural diversity, broad utility, and intrinsic degradability. Owing to the presence of hydrolyzable ester linkages, polyesters have long been regarded

as attractive alternatives to persistent polyolefin-based plastics and have found widespread applications in the packaging, commodity materials, engineering plastics, and biomedical fields.^{1–3} Conventionally, polyesters are synthesized either by the polycondensation of diols and dicarboxylic acids or by the ring-opening polymerization (ROP) of cyclic esters.^{4,5} In addition, the ring-opening copolymerization (ROCOP) of epoxides with cyclic anhydrides has emerged as an attractive approach for polyester synthesis.^{6–8} This approach offers good control of polymerization through a chain-growth mechanism as well as remarkable versatility in structural design by varying the combination of the epoxide and cyclic anhydride monomers. As a result, ROCOP provides a powerful platform for tuning polymer composition, functionality, and material properties and has developed into an important alternative to classical polyester synthesis.

Over the past several decades, numerous studies have focused on the development of new monomers. However, most of these efforts have primarily involved either introduction of specific side groups or utilization of new biomass-derived feedstocks.^{9–13} By contrast, relatively little attention has been

^aDivision of Applied Chemistry, Faculty of Engineering, Hokkaido University, Sapporo 060-8628, Japan. E-mail: feng.li@eng.hokudai.ac.jp, satoh@eng.hokudai.ac.jp

^bGraduate School of Chemical Sciences and Engineering, Hokkaido University, Sapporo 060-8628, Japan

^cGraduate School of Natural Science and Technology, Kanazawa University, Kakuma-machi, Kanazawa, 920-1192 Japan

^dFaculty of Biological Science and Technology, Institute of Science and Engineering, Kanazawa University, Kanazawa, 920-1192, Japan

^eNano Life Science Institute (WPI-NanoLSI), Kanazawa University, Kakuma-machi, Kanazawa, 920-1192 Japan

^fList Sustainable Digital Transformation Catalyst Collaboration Research Platform (ICReDD List-PF), Institute for Chemical Reaction Design and Discovery, Hokkaido University, Sapporo 001-0021, Japan

^gDepartment of Chemical & Materials Engineering, National Central University, Taoyuan 320317, Taiwan

[†]T. Gao and H. Ayakawa contributed equally to this study.



devoted to innovations in the fundamental substitution patterns of monomers. Taking epoxides as an example, monosubstituted epoxides and 1,2-disubstituted epoxides represent the most common substitution patterns employed in ROCOP with cyclic anhydrides (Fig. 1A). For 1,1-disubstituted epoxides, ROCOP using cyclic anhydrides and isobutylene oxide (IBO) has attracted research attention only recently.^{14–18} The bulky *gem*-dimethyl groups of IBO directly nucleophilically attack the less hindered methylene carbon, thereby favoring highly regular head-to-tail linkages. In addition, the symmetric structure of the polyesters synthesized from IBO facilitates regular chain packing, leading to semi-crystalline materials that are difficult to obtain using racemic monosubstituted epoxides or *meso*-1,2-disubstituted epoxides. Although these studies highlight the potential of 1,1-disubstituted epoxides in ROCOP, the reported examples are limited to IBO.

Spiro-epoxides, a special subclass of 1,1-disubstituted epoxides, have not been explored in ROP prior to our recent report describing the successful ROP of spiro-epoxide DBOO which was synthesized from cellulose-derived dihydrolevoglucosone (cyrene) in a single step.^{19,20} This polymerization afforded a biobased aliphatic polyether with an unexpectedly

high glass-transition temperature ($T_g = 140$ °C). This success encouraged us to further explore the potential of spiro-epoxides in other polymerization processes, particularly in the ROCOP with cyclic anhydrides (Fig. 1B). Given the unique structure of DBOO, ROCOP of its structurally related spiro-epoxides with cyclic anhydrides are expected to produce polyesters with previously unexplored backbone structures, thereby expanding the scope of ROCOP chemistry. This strategy represents a new approach for the utilization of cellulose-derived LGO/cyrene in polymer synthesis.^{21–24} Furthermore, the bulky and optically active nature of these epoxides may endow the resulting polyesters with regular chiral secondary structures.

In this study, we report the ROCOP of (dihydro)levoglucosone-derived spiro-epoxides, including DBOO and DBOOPh, with cyclic anhydrides. The resulting polyesters were investigated with regard to their material properties, including thermal properties and chiral secondary structures.

2. Results and discussion

2.1. ROCOP of DBOO and phthalic anhydride

Following a previously reported procedure, DBOO monomers were synthesized *via* the Corey–Chaykovsky reaction using Cyrene™. Depending on the type of ylide agent, DBOO with two different diastereomeric ratios (dr = 50:50 and 87:13) were obtained.^{19,20} They are referred to as DBOO_(50:50) and DBOO_(87:13), respectively.

ROCOP was initially performed using DBOO_(50:50) and phthalic anhydride (PA). 1,4-Benzenedimethanol (BDM) was used as an initiator. The investigation began with catalyst screening which was performed in bulk at 60 °C (Table 1, runs 1–4; Scheme S1; Fig. S1).

First, several different catalyst systems including *t*-BuP₂, 7-methyl-1,5,7-triazabicyclo[4.4.0]dec-5-ene (MTBD) organo-base catalysts, MTBD/triethylborane (TEB) acid/base binary catalysts, and cesium pivalate (CsOPiv), were tested within the same period of 20 h.^{25–27} The systems using *t*-BuP₂ and CsOPiv catalysts gave monomer conversions higher than 20%, while the MTBD and MTBD/TEB catalytic systems did not show sufficient reactivity, with a monomer conversion of no more than 10%. *t*-BuP₂ showed superior reactivity and controllability in the ROCOP of PA and isobutylene oxide (IBO), the most representative 1,1-disubstituted epoxide, in our previous report.¹⁷ However, *t*-BuP₂ does not outperform CsOPiv with regard to the reactivity. Moreover, when using *t*-BuP₂ as the catalyst, the polymerization system rapidly changed from colorless to black. Small unidentified peaks were observed in the crude ¹H NMR spectrum in contrast to that obtained using CsOPiv (Fig. S1). After identifying CsOPiv as the most suitable catalyst, the polymerization time was extended to obtain higher monomer conversion. As a result, after 120 h, PA conversion reached 79.6%, and the corresponding polymer was obtained with relatively narrow dispersity ($\bar{D} = 1.22$) (Table 1, run 5; Fig. S2). The poly(DBOO_(50:50)-*alt*-PA) structure was confirmed by ¹H NMR spectroscopy and MALDI-TOF MS, indicat-

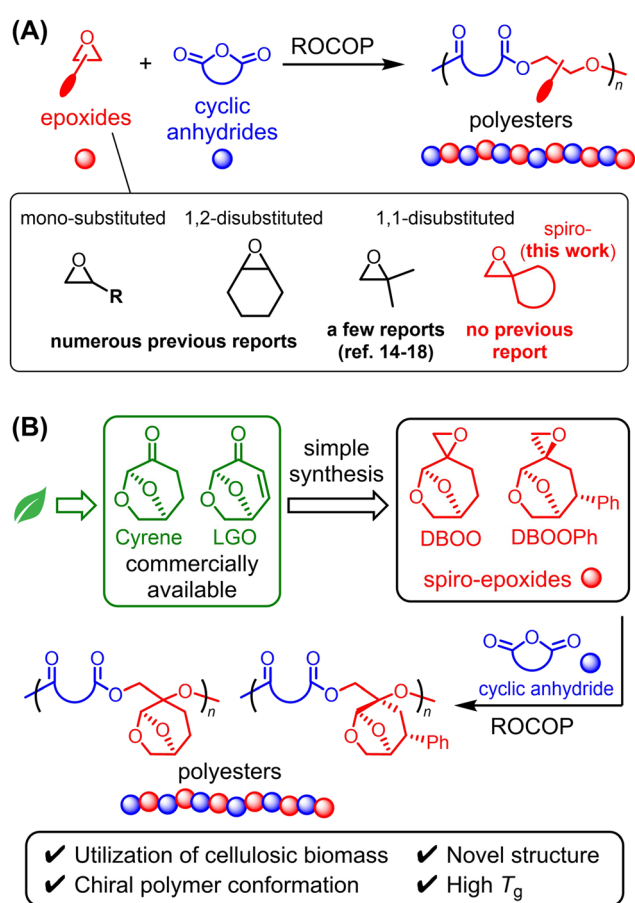
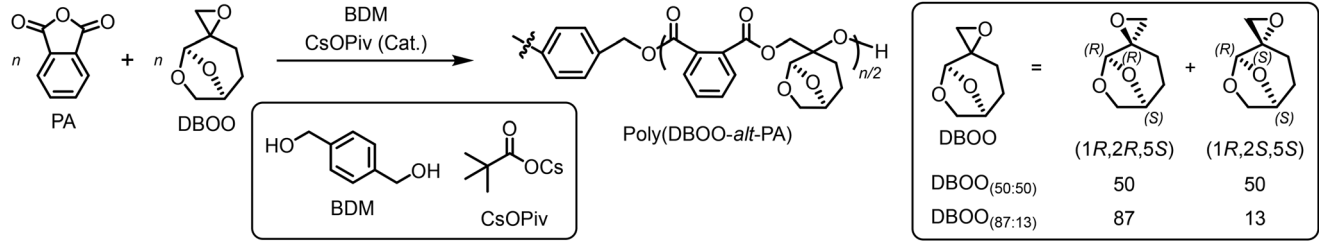


Fig. 1 (A) Ring-opening copolymerization of cyclic anhydrides and epoxides bearing different substitution patterns; (B) schematic illustration of this work.



Table 1 ROCOP of DBOO and phthalic anhydride^a


Run	Catalyst	[PA] ₀ /[DBOO] ₀ /[I] ₀ /[Cat.]	Temp. (°C)	Time (h)	Conv. _{PA} ^b (%)	M _{n,theo.} ^c	M _{n,NMR} ^b	M _{n,SEC} ^d	D ^d
1	<i>t</i> -BuP ₂	70/280/1/1	60	20	22	4500	n.d.	1100	1.31
2	MTBD	70/280/1/1	60	20	6	1400	n.d.	n.d.	n.d.
3	MTBD + TEB	70/280/1/1	60	20	10	2200	n.d.	n.d.	n.d.
4	CsOPiv	70/280/1/1	60	20	30	6100	n.d.	2000	1.28
5	CsOPiv	70/200/1/1	60	120	79.6	16 000	10 700	4400	1.22
6 ^e	CsOPiv	60/60/1/1	100	24	74.7	13 000	12 900	5200	1.16
7 ^e	CsOPiv	30/30/1/1	100	8	72.0	6200	6500	3300	1.14
8 ^e	CsOPiv	90/90/1/1	100	72	75.1	19 600	21 900	7500	1.14
9 ^{e,f}	CsOPiv	90/90/1/1	100	22.5	72.0	18 900	17 800	5700 ^g	1.31 ^g

^a Polymerization conditions: Ar atmosphere; BDM initiator. ^b Determined from ¹H NMR spectrum of the obtained polymer in CDCl₃. ^c Calculated from [PA]₀/[BDM]₀ × conv._{PA}/100 × ((M.W. of PA) + (M.W. of DBOO)) + (M.W. of BDM). ^d Determined by SEC of the polymer obtained in THF using a polystyrene standard. ^e n(PA) = 2.60 mmol, Vol(toluene) = 520 μL. ^f DBOO_(87:13) was used. ^g Determined by SEC (CHCl₃, polystyrene standard).

ing a perfectly alternating structure. No poly(DBOO) homopolymer or segments were observed (Fig. 2A and B). Although a small shoulder peak was observed in the SEC trace in the low-molecular-weight region, the molecular weight distribution remained relatively narrow. The low-molecular-weight shoulder peak was assigned to poly(DBOO_(50:50)-alt-PA), which was initiated by CsOPiv. As CsOPiv is a monofunctional initiator, it should result in a polymer with a molecular weight that is half of that of the polymer initiated by the difunctional initiator BDM. This is in agreement with the SEC trace observations.

Following the success of the DBOO/PA ROCOP in bulk, the solution polymerization in toluene with [PA]₀ = [DBOO]₀ was examined to fully exploit DBOO. Because the reduced monomer concentration resulting from the addition of solvent decreases the polymerization rate, the reaction temperature was increased to 100 °C to allow the reaction to reach completion within a reasonable time. To our delight, the polymerization proceeded well. The monomer conversion reached 74.7% after 24 h, and the theoretical molecular weight (M_{n,theo.}) and NMR molecular weight (M_{n,NMR}) matched well (Table 1, run 6). The obtained polymer exhibited a relatively narrow dispersity (D = 1.16). Polymerization with different target degrees of polymerization (DP) was examined by varying the [monomer]₀/[initiator]₀ ratio (Table 1, runs 7, 8). M_n increased with the feed ratio, and the dispersity remained narrow, further demonstrating the well-controlled nature of the polymerization (Fig. 2C).

When using DBOO_(87:13), which is a DBOO monomer with a different diastereomeric ratio, in the same solution polymerization conditions (Table 1, run 9), the obtained result was similar to that obtained using DBOO_(50:50). However, the obtained poly(DBOO_(87:13)-alt-PA) exhibited much lower solubi-

lity in THF than poly(DBOO_(50:50)-alt-PA), and its M_{n,SEC} (5.7 kDa) was measured in chloroform rather than in THF (Fig. S3). The ¹H NMR spectrum of poly(DBOO_(87:13)-alt-PA) exhibited different relative peak intensities from those of poly(DBOO_(50:50)-alt-PA) due to the different diastereomeric ratios of the monomers (Fig. S4 and S5).

In our previous study on the homopolymerization of DBOO, the two diastereomers exhibited different reaction rates, with the (1*R*,2*S*,5*S*)-diastereomer consumed approximately 1.6 times faster than the (1*R*,2*R*,5*S*)-diastereomer. To understand the reactivities of the two ROCOP diastereomers with PA, a kinetic monitoring experiment was conducted (Table S1; Fig. 2D and S6). It was found that the difference in the consumption rate between the two diastereomers of DBOO was much smaller than that in the ROP of DBOO (Fig. S7). This result demonstrated the nearly ideal random distribution of DBOO diastereomers along the poly(DBOO_(50:50)-alt-PA) polymer chain.

2.2. Monomer scope

Following the successful ROCOP of DBOO and PA, other monomer combinations were examined (Table 2). Based on our previous experience in the ROCOP of IBO and cyclic anhydrides, we selected glutaric anhydride (GA), diglycolic anhydride (DGA), and norbornene anhydride (NA) as the cyclic anhydride monomers to test the copolymerization with DBOO_(50:50), with the [cyclic anhydride]₀/[DBOO_(50:50)]₀/[BDM]/[CsOPiv] feed ratio fixed at 100/100/1/1 (Table 2, runs 1–3). The polymerizations using GA and DGA were performed in toluene at 100 °C. Similar to the reaction using PA which has a high target DP (Table 1, run 8), these two polymerizations required a comparably long reaction time to obtain high monomer con-



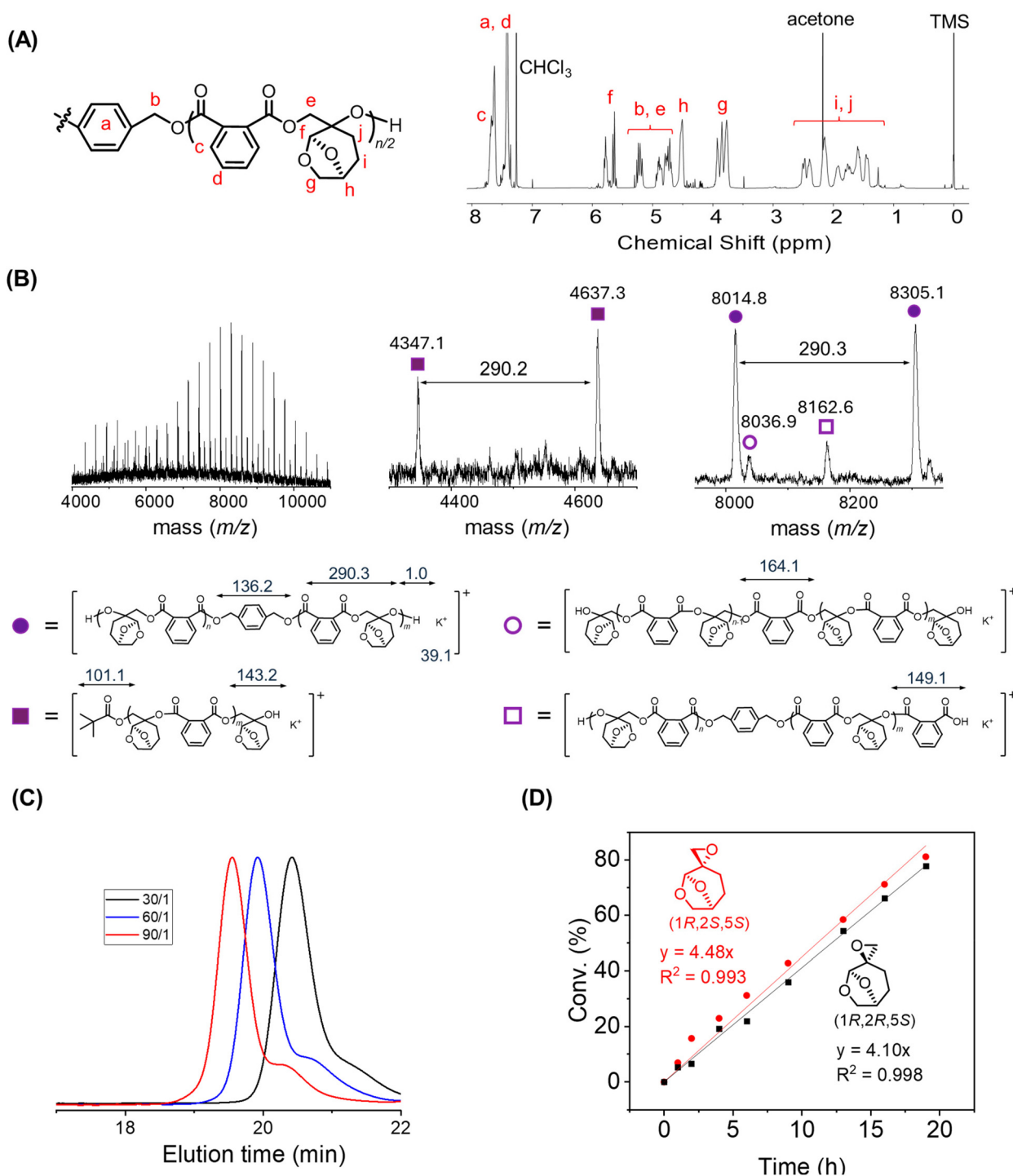


Fig. 2 (A) ^1H NMR spectra of poly(DBOO_(50:50)-alt-PA) (Table 1, run 5); (B) MALDI-TOF MS of poly(DBOO_(50:50)-alt-PA) (Table 1, run 5); (C) SEC trace of synthesized poly(DBOO_(50:50)-alt-PA) with different molecular weight (Table 1, run 6–8); (D) monomer conversion monitoring during ROCOP of PA and DBOO (Table S1).

version. In both cases, the $M_{n,\text{theo}}$ and $M_{n,\text{NMR}}$ values showed reasonable agreement. Although the dispersity values of the polymer were relatively narrow ($D = 1.18$ and 1.26), $M_{n,\text{SEC}}$ values were drastically lower than $M_{n,\text{NMR}}$. The alternating structures of the resulting polymers were confirmed by ^1H

NMR and MALDI-TOF MS (Fig. S8–S13). Multiple unidentified small peaks were observed in the MALDI-TOF MS spectra of both poly(DBOO_(50:50)-alt-GA) and poly(DBOO_(50:50)-alt-DGA), indicating the occurrence of undesired side reactions during polymerization.



Table 2 Conditions and results of ROCOP of various monomers^a

Run	Cyclic anhydride/epoxide	Temp. (°C)	Time (h)	Conv. ^b (%)	$M_{n, \text{theo.}}^c$	$M_{n, \text{NMR}}^b$	$M_{n, \text{SEC}}^d$	D^d
1	GA/DBOO _(50:50)	100	72	84.0	21 800	26 700	3000	1.18
2	DGA/DBOO _(50:50)	100	96	>99.9	26 100	27 200	3600	1.26
3	NA/DBOO _(50:50)	80	620	n.d.	n.d.	n.d.	2300	1.45
4	PA/DBOOPh	110	228	98.0	25 100	n.d.	3600	1.32

^a Polymerization conditions: [cyclic anhydride]₀/[epoxide]₀/[BDM]/[CsOPiv] = 100/100/1/1; Ar atmosphere; $n(\text{cyclic anhydride}) = 4.00 \text{ mmol}$, Vol (toluene) = 800 μL . ^b Determined from ¹H NMR spectrum of the obtained polymer in CDCl₃. ^c Calculated from [cyclic anhydride]₀/[BDM]₀ × conv._{DBOO}/100 × ((M.W. of cyclic anhydride) + (M.W. of DBOO)) + (M.W. of BDM). ^d Determined by SEC of the polymer obtained in THF using a polystyrene standard.

After examining GA and DGA, which are monocyclic anhydrides, tricyclic anhydride NA was tested in ROCOP with DBOO (Table 2, run 3). However, polymerization at 100 °C resulted in a polymer product with very broad dispersity ($D = 1.74$, Table S2, run 1). The product was improved by reducing the polymerization temperature to 80 °C ($D = 1.48$, Table S2, run 2). In contrast to the aforementioned polymerization systems, it was difficult to identify monomer conversion in NA/DBOO ROCOP using ¹H NMR because of peak overlap. Therefore, polymerization was performed for a long time (620 h) to ensure sufficient monomer conversion. As a result, the poly(DBOO_(50:50)-*alt*-NA) polymer was obtained with a $M_{n, \text{SEC}} = 2.3 \text{ kDa}$, and a slightly broader dispersity ($D = 1.45$, Table 2, run 3; Fig. S14 and S15). In the MALDI-TOF MS spectrum, although multiple peak series were observed, and some of these could not be identified, the periodic peak interval (306.3 Da) matched the sum of the molecular weights of NA and DBOO, supporting the formation of an alternating copolymer (Fig. S16).

After examining different cyclic anhydrides, we expanded the scope of cellulose-derived spiro epoxide monomers. In LGO, the α, β -unsaturated C=C double bond provides some opportunities to introduce an additional substituent. As a proof-of-concept, we synthesized DBOOPh *via* the introduction of a phenyl group using the well-known 1,4-addition of LGO, followed by the Corey–Chaykovsky reaction (Schemes S2 and S3). DBOOPh was obtained as a single diastereomer (Fig. S17–S20).

ROCOP of DBOOPh with PA was carried out at 110 °C due to the increased steric hindrance by the additional phenyl group (Table S3; Table 2, run 4). The monomer conversion

reached 98% after 228 h. Despite low reactivity, it afforded poly(DBOOPh-*alt*-PA) with $M_{n, \text{SEC}} = 3.6 \text{ kDa}$ and moderate dispersity ($D = 1.32$) (Fig. S21). The ¹H NMR spectrum and MALDI-TOF MS of the polymer further supported the alternating structure (Fig. S22 and S23).

2.3. Physical properties investigation

The thermal properties of the polymers obtained by the aforementioned polymerization were evaluated. First, thermogravimetric analysis (TGA) of the synthesized polyesters was performed. The 5% weight-loss decomposition temperatures ($T_{d, 5\%}$) were determined to be in the range of 224–297 °C, demonstrating sufficient thermal stability (Fig. S24–S29). Subsequently, the obtained polyesters were examined by differential scanning calorimetry (DSC) analysis (Fig. S30–S35). As summarized in Fig. 3, the glass-transition temperatures (T_g) of the polyesters ranged from 29 °C to 130 °C. In particular, poly(DBOO_(50:50)-*alt*-GA) and poly(DBOO_(50:50)-*alt*-DGA) exhibited relatively low T_g values of 29 °C and 64 °C, respectively, consistent with their incorporation of relatively flexible aliphatic segments in the backbone. The higher T_g of poly(DBOO_(50:50)-*alt*-DGA) compared to that of poly(DBOO_(50:50)-*alt*-GA) can be attributed to the presence of additional aliphatic ether moieties which result in additional interactions between the polymer chains. Introduction of bulky and rigid cyclic anhydride units restricted segmental motion, resulting in a much higher T_g of 130 °C for both poly(DBOO_(50:50)-*alt*-PA) and poly(DBOO_(50:50)-*alt*-NA).

For poly(DBOO_(87:13)-*alt*-PA) and poly(DBOOPh-*alt*-PA), more ordered structures were expected owing to the use of diastereomerically enriched and even optically pure monomers.





Fig. 3 DSC traces of synthesized polyesters.

However, no crystallization (T_c) or melting (T_m) transitions were detected in the DSC traces. The T_g of poly(DBOO_(87:13)-*alt*-PA) was found to be 127 °C, which is similar to that of poly(DBOO_(50:50)-*alt*-PA). The T_g for poly(DBOOPh-*alt*-PA) was measured as 123 °C, which is even slightly lower than that of poly(DBOO-*alt*-PA), despite the additional introduction of a rigid phenyl substituent. The amorphous nature of the obtained polyesters was further confirmed by X-ray diffraction (XRD) analysis (Fig. S36–S41).

2.4 Investigation of the secondary structure *via* circular dichroism

In our previous study on the ROP of DBOO, the resulting PDBOO polyether was expected to adopt a helical conformation when a single diastereomer or a diastereomerically enriched monomer was used.²⁰ However, experimental validation of this conformation proved difficult owing to the lack of the ultraviolet-visible (UV-VIS) absorption and poor solubility of poly(DBOO_(87:13)).

In the present study, for ROCOP with PA, the rigid benzene ring of PA together with the bulky spiro-epoxide monomers afforded polyesters with high glass transition temperatures, indicating relatively rigid backbone structures. Moreover, the chirality of DBOO or DBOOPh may induce the polymer chains to adopt chiral secondary conformations such as helices.

Taking advantage of the UV absorption arising from the aromatic ring, the UV-VIS absorption and circular dichroism (CD) spectra of poly(DBOO_(50:50)-*alt*-PA), poly(DBOO_(87:13)-*alt*-PA), and poly(DBOOPh-*alt*-PA) were measured in chloroform (Fig. 4 and S42). An absorption band attributed to the α -band of the aromatic rings in the polymer backbone was observed in

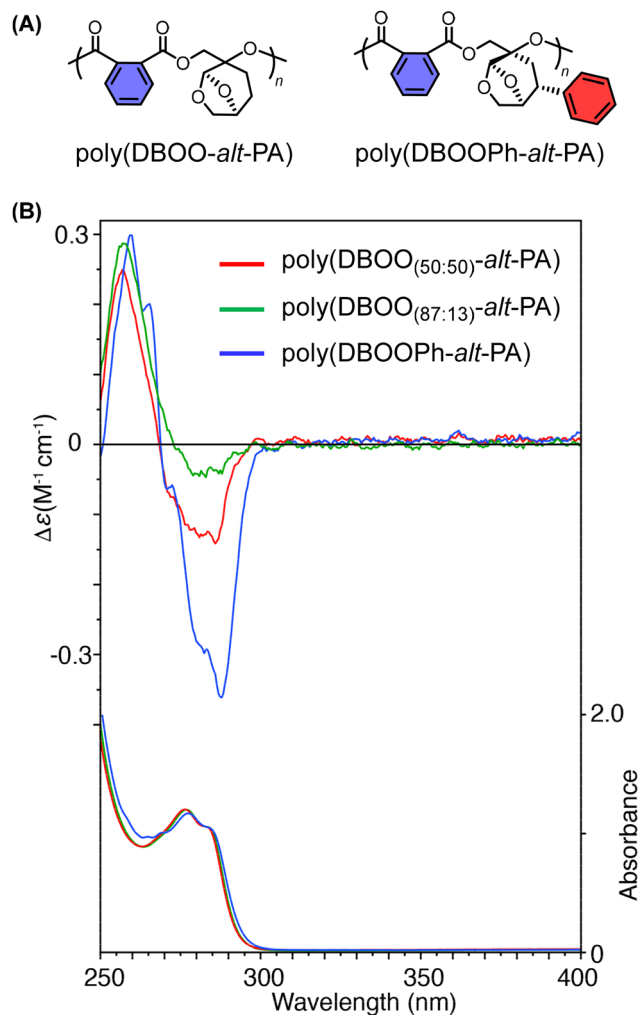


Fig. 4 (A) Chemical structures of poly(DBOO-*alt*-PA) and poly(DBOOPh-*alt*-PA) with highlighted benzene rings; (B) CD (top) and UV-vis absorption (bottom) spectra of poly(DBOO_(50:50)-*alt*-PA) (red), poly(DBOO_(87:13)-*alt*-PA) (green), and poly(DBOOPh-*alt*-PA) (blue) measured in chloroform at -20 °C ([polymer] = 10 mM, based on repeating units).

the region of 260–300 nm. For all polymers, the molar absorptivity (ϵ) at 270 nm was approximately $1200 \text{ L mol}^{-1} \text{ cm}^{-1}$, confirming that the absorption originated from the aromatic backbone.

The CD spectra of these three polymers exhibited a similar split Cotton effect in the region of 250–300 nm: the negative 1st Cotton, positive 2nd Cotton, and the cross point at approximately 270 nm. These results indicate that, regardless of the diastereomeric ratio of DBOO or the use of the DBOOPh monomer, the exciton coupling between aromatic units along the polymer chain preferentially adopts a counter-clockwise arrangement, which may induce a biased left-handed helical conformation. Among the three samples, the most distinct CD signal was observed for poly(DBOOPh-*alt*-PA), presumably due to the use of an optically pure epoxide monomer which further increased the rigidity by introducing a phenyl side group.



- 15 A. K. Hubbell, J. R. Lamb, K. Klimovica, M. Mulzer, T. D. Shaffer, S. N. MacMillan and G. W. Coates, *ACS Catal.*, 2020, **10**, 12537–12543.
- 16 L. Hu, X. Zhang, X. Cao, D. Chen, Y. Sun, C. Zhang and X. Zhang, *Macromolecules*, 2021, **54**, 6182–6190.
- 17 M. Sugiyama, R. Suzuki, H. Ayakawa, T. Gao, F. Li, T. Yamamoto, T. Isono and T. Satoh, *Polym. J.*, 2025, **57**, 1153–1163.
- 18 Z. Xie, Z. Yang, C. Hu, M. Niu, Y. Zhang, T. Yang, X. Pang and X. Chen, *Nat. Commun.*, 2026, **17**, 2668.
- 19 M. M. Zanardi, A. G. Suárez and A. M. Sarotti, *J. Org. Chem.*, 2017, **82**, 1873–1879.
- 20 H. Ayakawa, T. Nishimura, F. Li, T. Gao, T. Yamamoto, K. Tajima, T. Isono, K. Maeda and T. Satoh, *ACS Macro Lett.*, 2026, **15**, 725–731.
- 21 M. K. Stanfield, R. S. Terry, J. A. Smith and S. C. Thickett, *Polym. Chem.*, 2023, **14**, 4949–4956.
- 22 P. Ray, T. Hughes, C. Smith, M. Hibbert, K. Saito and G. P. Simon, *Polym. Chem.*, 2019, **10**, 3334–3341.
- 23 G. Wang, S. Ji, Z.-C. Li and C. Shi, *Chin. Chem. Lett.*, 2026, 112581.
- 24 Y. Mizukami, Y. Kakehi, F. Li, T. Yamamoto, K. Tajima, T. Isono and T. Satoh, *ACS Macro Lett.*, 2024, **13**, 252–259.
- 25 H. Li, J. Zhao and G. Zhang, *ACS Macro Lett.*, 2017, **6**, 1094–1098.
- 26 L.-F. Hu, C.-J. Zhang, H.-L. Wu, J.-L. Yang, B. Liu, H.-Y. Duan and X.-H. Zhang, *Macromolecules*, 2018, **51**, 3126–3134.
- 27 X. Xia, R. Suzuki, K. Takojima, D.-H. Jiang, T. Isono and T. Satoh, *ACS Catal.*, 2021, **11**, 5999–6009.

